Geo-Mar Lett
DOI 10.1007/s00367-016-0473-3

ORIGINAL

Observations of pockmark flow structure in Belfast Bay, Maine, Part 2: evidence for cavity flow

Christina L. Fandel[1,2] · **Thomas C. Lippmann**[1] · **Diane L. Foster**[1] · **Laura L. Brothers**[3]

Received: 5 April 2016 / Accepted: 25 September 2016

Abstract Pockmark flow circulation patterns were investigated through current measurements along the rim and center of two pockmarks in Belfast Bay, Maine. Observed time-varying current profiles have a complex vertical and directional structure that rotates significantly with depth and is strongly dependent on the phase of the tide. Observations of the vertical profiles of horizontal velocities in relation to relative geometric parameters of the pockmark are consistent with circulation patterns described qualitatively by cavity flow models (Ashcroft and Zhang 2005). The time-mean behavior of the shear layer is typically used to characterize cavity flow, and was estimated using vorticity thickness to quantify the growth rate of the shear layer horizontally across the pockmark. Estimated positive vorticity thickness spreading rates are consistent with cavity flow predictions, and occur at largely different rates between the two pockmarks. Previously modeled flow (Brothers et al. 2011) and laboratory measurements (Pau et al. 2014) over pockmarks of similar geometry to those examined herein are also qualitatively consistent with cavity flow circulation, suggesting that cavity flow may be a good first-order flow model for pockmarks in general.

✉ Thomas C. Lippmann
lippmann@ccom.unh.edu

[1] Center for Coastal and Ocean Mapping, University of New Hampshire, 24 Colovos Rd, Durham, NH 03824, USA

[2] Now with: Hydrographic Surveys Division, Office of Coast Survey, National Oceanic and Atmospheric Administration, 1315 East-West Hwy, Silver Spring, MD 20910, USA

[3] U.S. Geological Survey, 384 Woods Hole Rd, Woods Hole, MA 02543, USA

Introduction

Pockmarks are crater-like depressions in the seafloor that are globally distributed and ubiquitous in nearshore environments (e.g., Kelley et al. 1994). These depressions are believed to form from fluid and gas escape from underlying, unconsolidated sediment and range in size from a few meters to several kilometers in diameter (Hovland and Judd 1988). The interaction of currents with these seafloor depressions is poorly understood, but is of primary importance to circulation, mixing, sediment transport within and morphological evolution of pockmarks. Understanding the character of the flow in the vicinity of pockmarks could lead to improved estimations of faunal and nutrient dispersion patterns around pockmarks (Wildish et al. 2008) as well as better constrain sedimentation and erosion rate estimation within and around these prominent seafloor features (Pau and Hammer 2013).

The morphologies of pockmarks are often described as circular or elliptical (or elongated), or more quantitatively by the relative distance across the longest axis of the rim (L) to the depth from the rim to the bottom of the pockmark (D). The length-to-depth ratio (L/D) for most observed pockmarks ranges from 1–10 depending on the nature of the bottom conditions and the flow fields where they are located (Manley et al. 2004; Hammer et al. 2009; Brothers et al. 2011; Pau and Hammer 2013). L/D ratios can determine the nature of the flow patterns observed and are used as guiding parameters for numerical simulations (e.g., Brothers et al. 2011).

Several previous studies have investigated flow circulation within pockmarks. Manley et al. (2004) conducted a long-term field study over a nearly circular pockmark with L/D~10 in Burlington Bay, Vermont. Observations of strong, upward-directed vertical velocity events and flow recirculation within the pockmark are consistent with back-eddy formation or the

Published online: 04 October 2016

development of a cyclostrophic flow within the pockmark. Three-dimensional numerical modeling completed by Hammer et al. (2009) examined current flow over a pockmark (L/D~5.7) with similar dimensions to those found naturally in the Inner Oslofjord, Norway pockmark field. Modeled results show contour-following currents with strong upward-directed velocities in the center and along the downstream edge of the pockmark that conceptually agree with the cyclostrophic flow model proposed by Manley et al. (2004). Brothers et al. (2011) numerically modeled incompressible flow over a simplified pockmark in two and three dimensions. The results show both contour-following and recirculating flow patterns within the pockmark as the relative L/D ratio of the pockmark is altered, and indicate that pockmark flow circulation is strongly influenced by the geometry of the depression. Field observations by Pau and Hammer (2013) of horizontal currents (vertical velocities within the pockmarks were not measured in their study) above pockmarks in Oslofjord (L/D ~5.3 and 4.3) show diurnal variation with subsurface maxima attributed to swimming fish. Laboratory observations by Pau et al. (2014) over towed physical models of pockmarks with higher L/D ratio (~8) show flow streamlines that dip down into the pockmark depression at the leading edge and upwell out of the pockmark at the trailing edge, consistent with contour-following currents without recirculation within the pockmark. Finally, plausible scenarios for the development of pockmarks have been proposed based on seismic observations of paleo-stratigraphy, and include contour-following currents that form stagnation points (and eddies) on the upstream side internal to the pockmark (Kilhams et al. 2011).

In all of these studies, and often in nature, the morphology of pockmarks resembles that of cavities (or surface cutouts) along a boundary. Flow past such cavities results in an evolution of the bottom boundary layer that depends on the dimensions of the cavity, a feature of cavities that has been well studied in engineering fields (e.g., Rockwell and Naudascher 1978; Ashcroft and Zhang 2005, and many others) and examined theoretically, empirically, and with numerical models (e.g., Sarohia 1977; Rockwell and Naudascher 1978; Ahuja and Mendoza 1995). These studies reveal cavity flow circulation is strongly influenced by boundary layer thickness, free-stream velocity, turbulence, and the geometry of the cavity. In cavity flow, a shear layer forms as the overriding flow separates at the upstream rim of the cavity due to interactions with the depression. Typically, the time-mean behavior of the shear layer is used to characterize cavity flow, and is strongly dependent on the L/D ratio of the cavity.

Cavity flow can be grossly subdivided into two flow regimes: closed cavity flow and open cavity flow. Closed cavity flow predominantly occurs in shallow cavities (L/D>9) and is characterized by the shear layer flowing into the cavity, reattaching along the base, and then separating again before the downstream wall. The flow dips down into the cavity and progresses across and out the downstream side without recirculating within the cavity (like cyclostrophic flow patterns). Conversely, open cavity flow typically occurs in deeper cavities (L/D<6) and is described by the shear layer passing over the cavity and reattaching along the trailing edge (Fig. 1 shows a schematic that illustrates open cavity flow). In this case, a recirculation cell with overturning currents develops

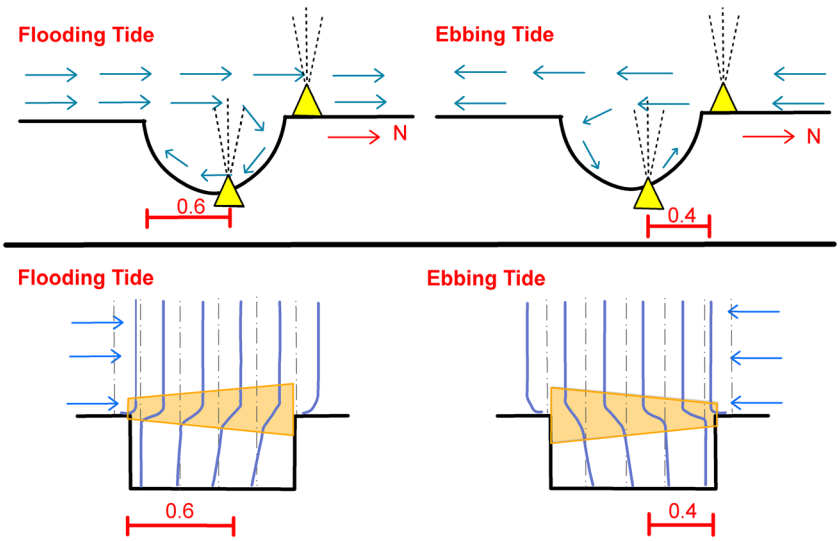

Fig. 1 Schematic model of open cavity flow circulation and shear layer growth with distance downstream. *Yellow triangles* Approximate location of ADCPs within the pockmark, *red* fractional distance (relative to L) downstream from the leading edge. *Top panel* Expected circulation patterns for open cavity flow during the flooding and the ebbing tides. *Bottom panel* Temporally varying horizontal velocity profiles across a modeled cavity during flooding and ebbing tidal conditions, and approximate shear layer growth with distance downstream (shaded *orange* region). The horizontal velocity profiles are offset based on position within the cavity with zero flow marked by a dash-dot *gray* line. Modified from Fig. 3 of Ashcroft and Zhang (2005)

across the cavity with center of rotation at some location not necessarily at the center. If the overturning cell is pushed to the downstream side of the cavity, measurements toward the leading edge but within the cavity will resemble closed cavity flow. Thus, the location relative to the leading edge of the cavity and the nature of the recirculation (if present) will be important to characterizing the nature of the flow.

In open cavity flows, the time-mean development of the shear layer increases with distance downstream and can be estimated using vorticity thickness (δ_ω), given by

$$\delta_\omega = \frac{U_2 - U_1}{\partial\langle U\rangle/\partial z|_{\max_z}} \quad (1)$$

where U_1 is the time-averaged velocity magnitude at the bed (assumed to be 0 m/s), U_2 is the time-averaged free-stream velocity magnitude, and the denominator characterizes the vertical (z-coordinate) gradient of the time-averaged velocity profile $\langle U\rangle$ at the top (or maximum vertical position, $\max_z$) of the shear layer (Ashcroft and Zhang 2005). This behavior is depicted schematically in Fig. 1 (following Ashcroft and Zhang 2005). The spatial and temporal evolution of the vorticity thickness can be estimated from observations of velocity profiles extending from the seabed to the top of the shear layer.

In Part 1 of this broader study (Fandel et al. 2016a), field observations show that active mixing and overturning occurred within two pockmarks in Belfast Bay, and the flow structure may possibly be influenced by roughness-induced form drag caused by upstream pockmarks. In this work (Part 2 of the study), the relationship between pockmark geometry and internal circulation patterns is examined, and a conceptual open cavity flow model following Ashcroft and Zhang (2005) is presented that is qualitatively consistent with recirculation patterns and downstream growth of the shear layer observed within the two sampled pockmarks. The maintenance of pockmarks by near-bed tidal currents is examined in Part 3 of the study (Fandel et al. 2016b).

Materials and methods

Bathymetric and current measurements were obtained in July 2011 along the rim and center of two pockmarks in Belfast Bay (see Fig. 1 of Part 1, Fandel et al. 2016a). The nearly circular, northern pockmark is located within 21 m water depth (surface to the rim), has a 45 m rim diameter, and has relief of 12 m (rim to bottom) giving a length-to-depth ratio of 3.7. The more elongated (elliptical), southern pockmark is located in 25 m water depth, has approximately 80 m major axis length (the minor axis length is 36 m), vertical relief of 17 m, and a major axis length-to-depth ratio of 4.7. The relatively small length-to-depth ratios of the northern ($L/D \approx 3.7$) and southern ($L/D \approx 4.7$) pockmarks suggest that circulation patterns within these depressions should qualitatively resemble open cavity flow.

Current velocities as a function of elevation above the bottom were measured by bottom-mounted acoustic Doppler current profilers (ADCP) located at the center and rim of each pockmark (described in Part 1; Fandel et al. 2016a). ADCPs within the pockmarks were positioned slightly north of the geometric center along the northeastern sidewall at a tilt angle of about 18–25°. At these tilt angles, current observations extend to within 2–4 m and 7–9 m of the surface for the northern and southern pockmarks, respectively (see Fandel et al. 2016a for a more detailed description). The slightly offset position to the center of each pockmark is a distinction important to the interpretation of the circulation pattern and growth of the shear layer across the pockmark that would be qualitatively predicted by cavity flow models.

Observations described in Part I show that currents have strong vertical structure and can be subdivided into three sections, the surface, middle, and deep water column delimited by the average depth of the thermocline, about 8 m below the surface, and the depth of the rim. Surface tidal flows range from 0–0.25 m/s and are modified by local wind-driven currents. During slack tides, reversal of flow near the bottom of each pockmark temporally leads the surface flow (see Figs. 9 and 10 of Fandel et al. 2016a), consistent with typical boundary layer behavior in the presence of a decelerating flow field where the weaker near-bottom flows have less inertia and respond more quickly to changes in the forcing (Kundu and Cohen 2008).

Results

The temporal evolution of the hourly averaged horizontal current rotational behavior with depth over the northern, more circular pockmark, and southern, more elongate pockmark is shown in Fig. 2. The rotational structure is generally tidally varying but has complex surface and deep flow patterns. Horizontal current directions have high temporal variability and rotate both clockwise and counterclockwise with depth in the upper water column. Currents in the mid water column shift 45–180° between flooding and ebbing currents, but are more uniformly behaved with depth. Below the rim, the currents change direction, sometimes 180° over just a few meters distance. This abrupt reversal in flow direction is consistent with open cavity flow with well-developed overturning recirculation cell (as depicted in Fig. 1). Currents typically show a greater degree of rotation during the ebbing tide than the flood.

Hourly averaged horizontal current direction profiles for the southern, more elliptical pockmark are shown in

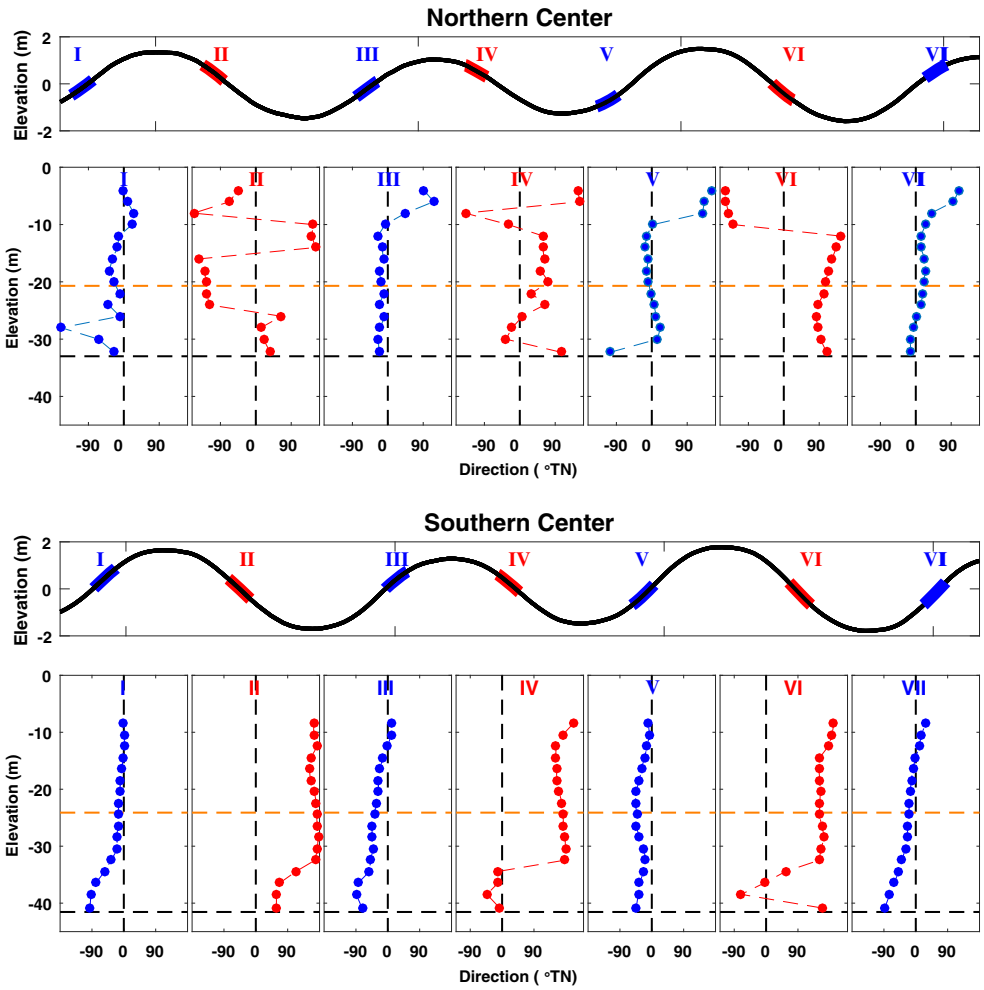

Fig. 2 Hourly averaged horizontal velocity direction profiles during maximum flooding (*blue*) and ebbing (*red*) tidal conditions from the center current meter mount in the northern (*top panel*) and southern (*bottom panel*) pockmark. Observed tidal oscillations are shown in the top panels with the horizontal axis progressing in time (same scale as in Fig. 3). Highlighted bars along the tidal cycle with representative roman numerals each correspond to the hourly averaged horizontal velocity direction profile shown in the *lower panels*. The horizontal axis of the lower panel denotes current direction where 0° (northerly flow) is marked by a vertically dashed gray line. The horizontally dashed *orange* and *black* lines in the lower panels denote the rim and bottom pockmark depth, respectively

the bottom panel of Fig. 2. A similar, tidally varying rotational pattern is observed but with less vertical and temporal variability than for the more circular northern pockmark. Directional changes from surface to depth typically rotate in a counterclockwise direction on the order of 90–180° during the ebbing tide and 50–90° during the flooding tide. Above the rim, near-northerly directed flow occurs during maximum flood tide and reverses nearly 180° during maximum ebb. In general, the depth-varying behavior in the mid to upper water column is much more uniform than for the northern pockmark, perhaps due to the stronger and more uniform currents in the narrow region of Belfast Bay. Below the rim, significant and abrupt changes in horizontal current direction are observed during the ebbing tide. This flow structure is consistent with open cavity flow with distinct vertical recirculation (Fig. 1). During the flooding tide, directional change below the rim is not as strong, and occurs more gradually. Flow reversals, when observed, occur below the rim typically at about 10 m above the seafloor, approximately midway between the rim and bottom of the pockmark.

Vorticity thickness was estimated from Eq. 1 using observations of the free-stream velocity magnitude, U_2, and the mean velocity gradient at the top of the shear layer, $\partial\langle U\rangle/\partial z|_{\max_z}$. Calculations of vorticity thickness, δ_ω, are separated into two categories (based on length scale) determined by the relative location of the current meter mount with respect to the leading edge of the pockmark during the flooding ($0.6L$) and ebbing ($0.4L$) tide, where L is the diameter (or major axis) at the rim.

The observed temporal evolution of the horizontal current magnitudes above the pockmark rim (top panels) for the northern and southern pockmarks are shown in Fig. 3. The dashed gray lines outline the upper 8 m of the water column delimiting the depth range over which the maximum velocity was determined and denoted as the free-stream velocity (U_2). Also shown is the evolution of the velocity gradient over depth calculated from the hourly averaged horizontal velocities acquired by the center mounted ADCP (middle panels). The gray circles denote the maximum gradient within the observed shear layer, outlined by the range bars that indicate the depths over which the velocity gradient was estimated. The calculated

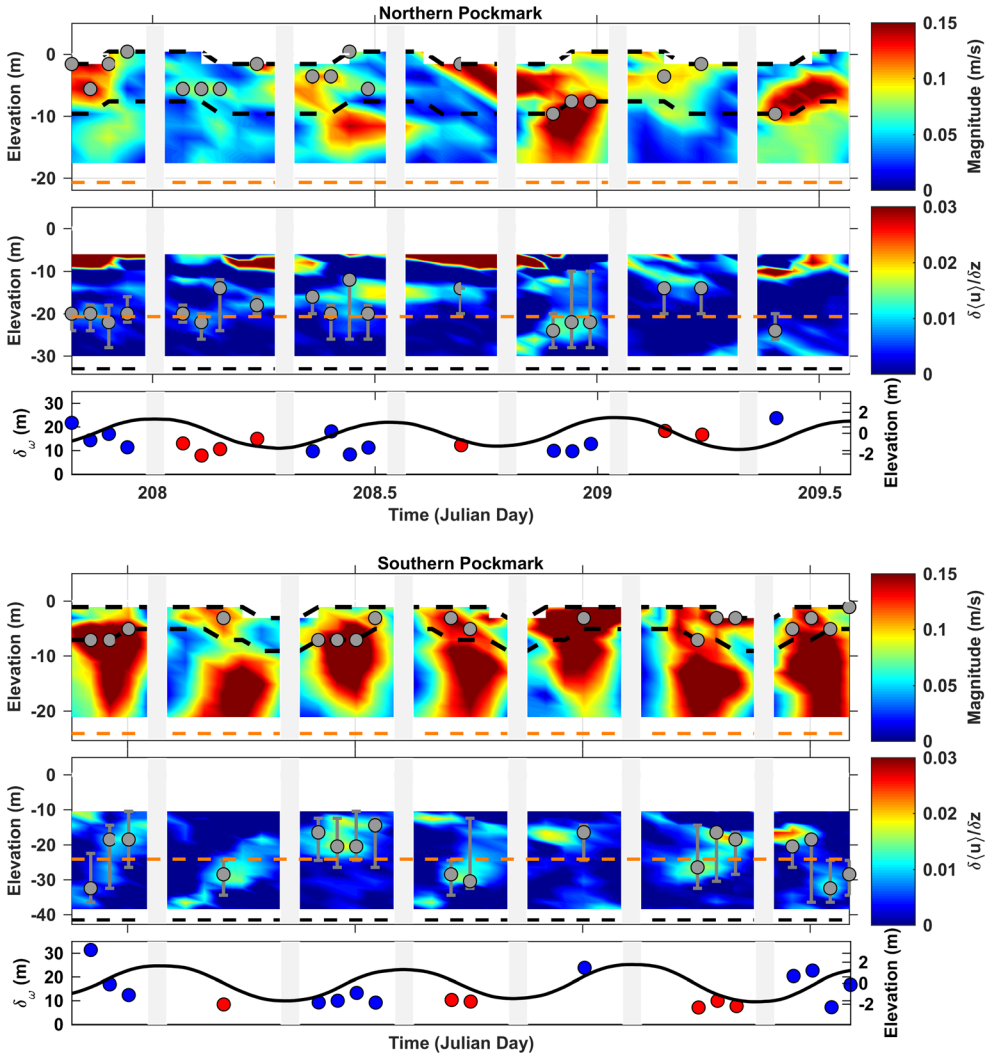

Fig. 3 Horizontal velocity magnitudes, mean horizontal velocity gradient over depth, and vorticity thickness for the northern (*top panel*) and southern (*bottom panel*) pockmark. The horizontal axis denotes time in Julian days, and the vertical axis is elevation relative to mean sea level where the *orange* and *black* dashed lines in the upper two panels denote the rim and bottom pockmark depth, respectively. The upper panel shows current magnitude data acquired at the rim. Dashed *gray* lines outline the upper 8 m of the water column from which a maximum velocity was chosen and denoted as the free-stream velocity (*gray dot*). The middle panel shows the observed vertical velocity gradient over the center of the pockmark, with the maximum gradient in velocity within the shear layer marked by a *gray* dot. Vertical lines across the dots denote the depth range over which the shear layer was defined. The *lower panel* shows estimated vorticity thicknesses during the flooding (*blue*) and ebbing (*red*) tide and are overlain by tidal observations. Note vorticity thickness was only estimated when a shear layer was observed in the hourly averaged velocity profile, and was not estimated during slack tide

vorticity thickness, δ_ω, is shown in the bottom panels overlain by the observed tidal oscillations. At slack tides the flow is zero and consequently the vorticity thickness cannot be estimated (denoted by blank regions in each panel).

The spreading rate ($\partial\delta_\omega/\partial x$) at which the estimated vorticity thickness increased across the pockmark largely differed between the two pockmarks. Mean vorticity thickness at the northern pockmark increased from 13.34 m during ebb tidal flow to 13.95 m during flood tidal flow at a spreading rate of 0.061. The estimated growth of the mean shear layer over the southern pockmark was much greater (0.36) and nearly doubled from ebbing (8.62 m) to flooding (16.07 m) tidal conditions.

Discussion

The complexity of the horizontal velocity structure over the northern and southern pockmarks may be partly due to the geographic location of the pockmarks within the bay (see Fig. 1 of Fandel et al. 2016a). Relatively higher velocity tidal flow enters Belfast Bay through a narrow channel to the west of Islesboro Island. The proximity of the southern pockmark to this channel yields more strongly tidally driven current observations than over the northern pockmark where increased complexity in horizontal current structure may be attributed to converging tidal currents around Islesboro Island (Xue and Brooks

2000). Depth-varying velocity structure is also partially due to the influence of the bottom boundary layer on tidally modulated flows (such as those described in Prandle 1982). In any case, the vertically varying rotational structure observed over the pockmarks shows abrupt directional changes during the ebbing tide that are consistent with that expected for open cavity flow and the formation of a recirculation cell within the pockmark (Rockwell and Naudascher 1978).

Recirculation cell formation is also observed over steeply sloped sand dunes (e.g., Paarlberg et al. 2009; Lefebvre et al. 2014a) and deep cavities (e.g., Ashcroft and Zhang 2005), but neither distinctly mimic the near-conical shape that characterizes pockmark geometry. Similar to pockmarks, cavities are defined by a base surrounded by four walls, but exhibit vertical sidewalls unlike the sloped sidewalls of pockmarks. Compa ratively, sand dunes share the sloping sidewall characteristic with pockmarks, but are defined as long linear features on the seabed and are not confined on all sides. Previous studies of flow over sand dunes show the formation of a flow separation zone, resulting in a recirculating cell that is followed by a turbulent wake downstream (Lefebvre et al. 2014b). A permanent flow separation zone (not observed in Ashcroft and Zhang 2005) is often observed over bedforms with a leeside slope equal or close to the angle of repose (30°; Bennett and Best 1995; Venditti and Bennett 2000; Lefebvre et al. 2014a). Given the steep sidewall angles of the sampled pockmarks (up to 60°) and observations of flow reversal near the bed during ebbing tidal conditions, it is possible that a flow separation zone followed by a turbulent wake region may describe the flow circulation within the sampled pockmarks. However, the spatial resolution of the fixed ADCP data is insufficient to accurately define the position and extent of the flow separation zone. Conversely, the applicability of the cavity flow model to the pockmark flow circulation may be assessed by examining the time-mean vorticity thickness across the sampled pockmarks.

The locations of the ADCPs within the pockmark are not centered, and thus yield different distances (over which shear layers can grow) relative to the direction of the tidal flows. The general circulation patterns for open cavity flow are illustrated in the diagram in Fig. 1, as well as the approximate shear layer growth with distance downstream of the leading edge of the pockmark. Observed vorticity thicknesses over both pockmarks are larger during flooding tidal conditions (Fig. 3), consistent with the expectation that for open cavity flow the shear layer grows with distance downstream.

Spreading rate estimates across the sampled pockmarks are qualitatively compared to those obtained by Ashcroft and Zhang (2005) over a modeled deep cavity (L/D=4; Fig. 4). Ashcroft and Zhang (2005) observed linear shear layer growth across the modeled cavity at a spreading rate of 0.14. The variability in spreading rates observed over the modeled deep cavity and the sampled pockmarks (northern $\partial\delta_\omega/\partial x = 0.061$ and southern $\partial\delta_\omega/\partial x = 0.36$) may be attributed to the geometric differences between these depressions, their relative proximity to converging currents or narrowing of the channel width, or the time variability associated with the natural flow field (consisting primarily of tides and wind-driven currents). In Ashcroft and Zhang (2005), modeled cavity geometry is described by vertical sidewalls and a flat bottom, whereas the Belfast pockmarks were conical in nature with an approximate 30–60° sidewall slopes (Fandel et al. 2016a). The influence of non-vertical sidewalls as well as proximity and possible influence of flow over other regional cavities (form drag; Fandel et al. 2016a)

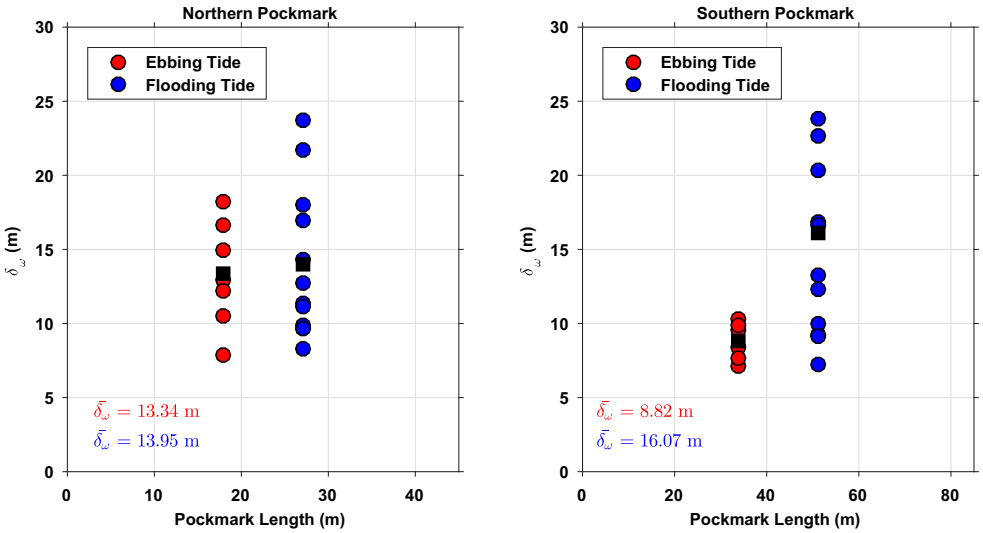

Fig. 4 Vorticity thickness relative to distance (in m) from the leading edge of the pockmark (denoted Pockmark Length in the panels) relative to the flow direction estimated over the northern and southern pockmark during flooding (*blue*) and ebbing (*red*) tidal conditions. Mean vorticity thicknesses during flooding and ebbing tidal conditions are represented as *black* squares with values indicated in the lower left corner of each graph

are unaccounted for in this model and may be responsible for some of the differences in spreading rate estimates. Although large variability in spreading rates were observed over the sampled pockmarks, observations of flow reversal near the base of the pockmarks and downstream growth of the shear layer are also consistent with open cavity flow, and suggest that cavity flow may describe the nature of flow circulation in the pockmarks of Belfast Bay.

The cavity flow model predicts varying circulation patterns depending on the geometry of the depression, often expressed as a function of the length-to-depth ratio. In shallow cavities (L/D>9), the shear layer typically reattaches along the base of the cavity and then separates again before the downstream edge, whereas in deep cavities (L/D<6) the shear layer extends across the cavity and then reattaches along the downstream wall. Referencing these length-to-depth thresholds, results from previous studies investigating flow circulation within pockmarks are qualitatively consistent with the cavity flow model. Hammer et al. (2009) conducted three-dimensional numerical simulations of flow within a pockmark (L/D=5.7) and found contour-following horizontal velocity currents that decreased in magnitude with depth, representative of closed cavity flow. While closed cavity flow is typically associated with cavities of L/D>9, the proximity of the length-to-depth ratio of the modeled pockmark to the theoretical threshold of open cavity flow (L/D<6) may account for the difference between the results of Hammer et al. (2009) and those found herein (with L/D=3.7 and L/D=4.7 for the two pockmarks sampled). Pau et al. (2014) conducted laboratory measurements of flow within a pockmark with L/D=8 that showed flow patterns without recirculation, consistent with closed cavity flow.

Numerical simulations conducted by Brothers et al. (2011) examined circulation patterns arising from two-dimensional turbulent flow over a shallow pockmark (L/D≈18) and three-dimensional laminar flow over a deep pockmark (L/D≈4.7). Modeled results indicate contour-following currents within the shallow pockmark and the formation of a large circulation cell within the deep pockmark that bridges the pockmark opening and circulates throughout the depression. These results are consistent with cavity flow circulation that predicts contour-following currents in shallow (L/D>9) cavities and recirculation cell formation within deep cavities (L/D<6).

Conclusions

Horizontal current direction profiles acquired within two pockmarks in Belfast Bay show significant rotation with depth and are tidally modulated, particularly below the rim. During the flooding tide, nearly northward surface currents gradually rotate 75±25° with depth. Larger directional changes are observed during ebbing tidal flow on the order of 180±50° and typically occur abruptly around 10 m from the bottom. The reversal of flow direction with depth during ebbing tidal conditions is qualitatively consistent with recirculation patterns predicted by open cavity flow (consistent with Ashcroft and Zhang 2005).

Shear layer growth rates that characterize the downstream spreading of high vorticity regions were approximated using vorticity thickness and are positive across both pockmarks. The near-bed flow reversal and shear layer growth with distance downstream are consistent with open cavity flow patterns (L/D<6) and suggest that pockmark flow circulation in Belfast Bay is reasonably well described by cavity flow. The consistency of observations presented herein with modeled and empirical results from previous Belfast Bay (Brothers et al. 2011) and Oslofjord (Hammer et al. 2009; Pau et al. 2014) studies indicate that cavity flow circulation (closed or open) may be a good first-order flow model for pockmarks in general.

Current observations made herein and those of others (Brothers et al. 2011; Pau et al. 2014) are qualitatively consistent with cavity flow whereby shallow cavities are defined by contour-following currents and deep cavities exhibit a recirculation cell within the depression. Other flow models, such as flow over steep-faced sand dunes, show similar circulation patterns; however, the resolution of the field observations obtained in this study is insufficient to verify the correlation between pockmarks and dune flow structure. Future work should include three-dimensional modeling of flow over pockmarks and model validation using more comprehensive field observations that span the pockmark (if possible). Such coincident fine-resolution modeling and field observations would lead to improved understanding of the primary and secondary flow structures within these depressions, as well as better relate pockmark flow circulation to that over cavities, sand dunes, or similar seafloor structures.

Acknowledgements Data obtained in this study are available at the Center for Coastal and Ocean Mapping, University of New Hampshire under the experiment name “2011 Belfast Bay Pockmark Experiment”. J. Kelley of the University of Maine provided the multibeam bathymetry map from which candidate pockmarks were identified for further study. This work was based upon a model conceived by P. Koons at the University of Maine and the many observations and interpretations made by J. Kelley, D. Belknap (University of Maine), W. Barnhardt (USGS) and B. Andrews (USGS). Field assistance was provided by J. Irish, Capt. E. Terry, Capt. B. Smith, and J. Hunt. Comments by J. Irish, T. Karla, and the anonymous reviewers greatly improved the manuscript. This research was supported by the National Oceanic and Atmospheric Administration under NOAA grant NA10NOS4000073. Any use of trade, firm, or product names is for descriptive purposes only and does not imply endorsement by the U.S. Government.

Compliance with ethical standards

Conflict of interest The authors declare that there is no conflict of interest with third parties.

References

Ahuja K, Mendoza J (1995) Effects of cavity dimensions, boundary layer, and temperature on cavity noise with emphasis on benchmark data to validate computational aeroacoustic codes. NASA Contractor Report NASA CR 4653

Ashcroft G, Zhang X (2005) Vortical structures over rectangular cavities at low speed. Phys Fluids 17:1–8

Bennett SJ, Best JL (1995) Mean flow and turbulence structure over fixed, two-dimensional dunes: implications for sediment transport and bedform stability. Sedimentology 42:491–513

Brothers LL, Kelley JT, Belknap DF, Barnhardt WA, Koons PO (2011) Pockmarks: self-scouring seep features? In: Proc 7th Int Conf Gas Hydrates, 17–20 July, Edinburgh, UK

Fandel CL, Lippmann TC, Irish JD, Brothers LL (2016a) Observations of pockmark flow structure in Belfast Bay, Maine, Part 1: current-induced mixing. Geo-Mar Lett, this volume. doi:

Fandel CL, Lippmann TC, Foster DL, Brothers LL (2016b) Observations of pockmark flow structure in Belfast Bay, Maine, Part 3: implications for sediment transport. Geo-Mar Lett, this volume. doi:

Hammer Ø, Webb KE, Depreiter D (2009) Numerical simulation of upwelling currents in pockmarks, and data from the Inner Oslofjord, Norway. Geo-Mar Lett 29:269–275

Hovland M, Judd AG (1988) Seabed pockmarks and seepages: Impact on geology, biology, and the marine environment. Graham and Trotman, London

Kelley JT, Dickson SM, Belknap DF, Barnhardt WA, Henderson M (1994) Giant sea-bed pockmarks: evidence for gas escape from Belfast Bay. Geology 22:59–62

Kilhams B, McArthur A, Huuse B, Ita E, Hartley A (2011) Enigmatic large-scale furrows of Miocene to Pliocene age from the central North Sea: current-scoured pockmarks? Geo-Mar Lett 31:437–449

Kundu P, Cohen I (2008) Fluid mechanics, 4th edn. Elsevier Academic Press, Burlington

Lefebvre A, Paarlberg AJ, Ernstsen VB, Winter C (2014a) Flow separation and roughness lengths over large bedforms in a tidal environment: a numerical investigation. Cont Shelf Res 91:57–69

Lefebvre A, Paarlberg A, Winter C (2014b) Flow separation and shear stress over angle of repose bedforms: a numerical investigation. J Water Resour Res 50:986–1005

Manley PL, Manley TO, Watzin MC, Gutierrez J (2004) Lakebed pockmarks in Burlington Bay, Lake Champlain: I. Hydrodynamics and implications of origin. In: Manley TO, Manley PL, Mihuc TB (eds) Lake Champlain: Partnerships and research in the new millennium. Springer, Berlin, pp 299–330

Paarlberg AJ, Dohmen-Janssen CM, Hulscher SJMH, Termes P (2009) Modeling river dune evolution using a parameterization of flow separation. J Geophys Res 114, F01014. doi:10.1029/2007JF000910

Pau M, Hammer O (2013) Sediment mapping and long-term monitoring of currents and sediment fluxes in pockmarks in the Oslofjord, Norway. Mar Geol 346:262–273

Pau M, Gisler G, Hammer Ø (2014) Experimental investigation of the hydrodynamics in pockmarks using particle tracking velocimetry. Geo-Mar Lett 34:11–19

Prandle D (1982) The vertical structure of tidal currents and other oscillatory flows. Cont Shelf Res 1:191–207

Rockwell D, Naudascher E (1978) Review - self-sustaining oscillations of flow past cavities. J Fluids Eng 100:152–165

Sarohia V (1977) Experimental investigation of oscillations in flows over shallow cavities. Am Inst Aero Astro J 15:984–991

Venditti JG, Bennett SJ (2000) Spectral analysis of turbulent flow and suspended sediment transport over fixed dunes. J Geophys Res 015: 22,035–22,047

Wildish DJ, Akagi HM, McKeown DL, Pohle GW (2008) Pockmarks influence benthic communities in Passamaquoddy Bay, Bay of Fundy, Canada. Mar Ecol Prog Ser 357:51–991

Xue H, Brooks D (2000) Characterization of fronts and eddies in Penobscot Bay using a three-dimensional ocean circulation model. Final Report presented to Island Institute, Rockland, ME